Raman scattering investigation across the magnetic and metal-insulator transition in rare earth nickelate $RNiO_3$ (R=Sm, Nd) thin films

C. Girardot,[1,2] J. Kreisel,[1,*] S. Pignard,[1] N. Caillault,[2] and F. Weiss[1]

[1]*Laboratoire des Matériaux et Génie Physique, CNRS, Grenoble Institute of Technology, Minatec 3, Parvis Louis Néel, 38016 Grenoble, France*

[2]*Schneider Electric Industries S.A.S., 37 Quai Paul Louis Merlin, 38050 Grenoble Cedex 9, France*

(Received 23 June 2008; published 2 September 2008)

We report a temperature-dependent Raman scattering investigation of thin-film rare earth nickelates $SmNiO_3$, $NdNiO_3$, and $Sm_{0.60}Nd_{0.40}NiO_3$ which present a metal-to-insulator (MI) transition at T_{MI} and an antiferromagnetic-paramagnetic Néel transition at T_N. Our results provide evidence that all investigated samples present a structural phase transition at T_{MI} but the Raman signature across T_{MI} is significantly different for $NdNiO_3$ ($T_{MI}=T_N$) compared to $SmNiO_3$ and $Sm_{0.60}Nd_{0.40}NiO_3$ ($T_{MI}\neq T_N$). It is namely observed that the paramagnetic-insulator phase ($T_N<T<T_{MI}$) in $SmNiO_3$ and $Sm_{0.60}Nd_{0.40}NiO_3$ is characterized by a pronounced softening of one particular phonon band around 420 cm^{-1}. This signature is unusual and points to an important and continuous change in the distortion of NiO_6 octahedra (thus the Ni-O bonding) which stabilizes upon cooling at the magnetic transition. The observed behavior might well be a general feature for all rare earth nickelates with $T_{MI}\neq T_N$ and illustrates intriguing coupling mechanism in the $T_N<T<T_{MI}$ regime.

DOI: 10.1103/PhysRevB.78.104101 PACS number(s): 63.20.−e, 73.61.−r, 64.70.kp, 77.80.Bh

I. INTRODUCTION

Rare earth nickelates with the generic formula $RNiO_3$ (R=rare earth) have attracted a lot of research interest since the report of a sharp metal-to-insulator (MI) transition whereof the critical temperature T_{MI} can be tuned with the rare earth size. Further to this, in the insulating phase most R nickelates exhibit a complex antiferromagnetic ordering below the Néel temperature T_N. Depending on the R, these two transitions occur either at the same temperature or they are distinct.[1–4]

For a long time the crystal structure of R nickelates was thought to be orthorhombic (space group *Pbnm*) in both the metallic and the insulator regimes and the understanding of the MI transition remained somehow puzzling.[2,3] This view has been challenged by neutron diffraction and high-resolution synchrotron diffraction experiments which reveal two distinguishable NiO_6 octahedra in the insulator phase of $RNiO_3$ leading to a monoclinic distortion with space group $P2_1/n$.[5,6] The observation of two independent Ni positions has been interpreted by the presence of a long-range charge disproportion ($2Ni^{3+}\rightarrow Ni^{3+\delta}+Ni^{3-\delta}$) in the insulating regime, while nickel is uniformly trivalent in the metallic regime.[5] Recently, several authors[4,7,8] have proposed that the charge order in the insulating regime might induce improper ferroelectricity, thus multiferroicity, but this theoretical prediction is not yet experimentally verified. The charge-disproportion scenario has been supported by a number of studies (e.g., Refs. 9 and 10) although other authors suggest a segregation into primarily ionic and primarily covalent bonding rather than charge transfer between the two Ni sites.[11] Further to this, there is increasing evidence that R nickelates present local deviations from the average crystal structure. However, their electric, magnetic, or structural nature is not yet clear and several scenarios such as two-phase and bond fluctuations[11–13] or a short-range charge order even in the metallic state[14] have been suggested. It is usually assumed that both the low-temperature monoclinic charge disproportion-type distortion and the short-range order are shared by all members of the $RNiO_3$ family and thus lead to a common mechanism of the MI transition independently if $T_{MI}=T_N$ or $T_{MI}\neq T_N$.

In this paper two R nickelates have been investigated: $SmNiO_3$ and $NdNiO_3$. These two nickelates are particularly interesting to compare because for $NdNiO_3$ the magnetic and MI transitions occur according to literature at the same temperature ($T_{MI}=T_N\approx-80$ °C) while they are distinct for $SmNiO_3$ ($T_{MI}\approx125$ °C, $T_N\approx-100$ °C) and this although the ionic radii of Nd^{3+} and Sm^{3+} differ by only 0.03 Å. Furthermore, T_{MI} can be readably adjusted[15] by varying x in $Sm_{1-x}Nd_xNiO_3$ and our comparison has thus been extend by the composition $Sm_{0.60}Nd_{0.40}NiO_3$ which has a MI transition near room temperature thus offering a promising suitability for applications.

The aim of our paper is threefold: (i) to verify if $SmNiO_3$ presents a symmetry breaking at the MI transition, knowing that such a symmetry breaking is not observed by high-resolution diffraction, (ii) to investigate if the mechanisms at the MI transition is driven by the same structural phase transition at T_{MI} for $T_{MI}=T_N$ and $T_{MI}\neq T_N$ systems, and (iii) to investigate if the phonon signature is notably affected by the magnetic and electric transitions.

In order to address the above questions, we have used Raman spectroscopy which is known to be a versatile technique for the investigation of thin-film oxides and in particular for the detection of even subtle structural distortions in perovskites.[16–20] Phonons are also known to be influenced by spin and electronic correlations thus offering a complementary tool for understanding transition-metal oxides.

II. EXPERIMENTAL DETAILS AND SAMPLE CHARACTERIZATION

The preparation of $RNiO_3$ materials in bulk form is difficult due to the necessity of an important oxygen pressure to

stabilize Ni in its 3+ state of oxidation.[1] A way to circumvent this difficulty is to stabilize $R\mathrm{NiO}_3$ by epitaxial strain in thin-film growth.[15,18,21] Most of the used deposition techniques, such as pulsed laser deposition, also need high oxygen pressure in order to fabricate the targets. On the other hand, a low-pressure metal-organic chemical vapor deposition (MOCVD) process offers an opportunity[21] to obtain $R\mathrm{NiO}_3$ phases without using high oxygen pressures. Here, we have used an 1:1 Ar-O_2 ratio at a pressure of 10 mbar with a flux of 600 $\mathrm{cm}^3/\mathrm{min}$. Nevertheless, $R\mathrm{NiO}_3$ can be only synthesized by MOCVD on cubic or pseudocubic single crystalline substrates presenting a lattice parameter close to that of the nickelate. It is then the stress imposed by the substrate to the film which leads to the thermodynamic stabilization of the nickelate phase.

Our thin films were obtained by injection metal-organic chemical vapor deposition "band flash" using 2,2,6,6-tetramethylheptanedionato-chelates of corresponding metals as volatile precursors. Polished single crystalline substrates of perovskite-type (00l) LaAlO_3 (LAO) was used to achieve an epitaxial stabilization of the films. Deposition conditions were 680 °C using an atmosphere of argon-oxygen at 10 mbar pressure followed by an *in situ* annealing during 30 min at ambient pressure under a pure oxygen flow. It has been previously reported that this technique and conditions lead to good quality *R*-nickelate thin films on various substrates.[22–25]

The thickness and chemical composition of the films were determined by wavelength dispersive spectroscopy (WDS) using a CAMECA SX50 spectrometer. A slight excess of Ni is measured corresponding to a minor NiO (220) oriented phase which is detected by x-ray diffraction on a Siemens diffractometer in a $\theta/2\theta$ geometry with a Cu anode ($\lambda = 1.5406$ Å). Furthermore, x-ray diffraction indicates that the SmNiO_3 (SNO), $\mathrm{Sm}_{0.60}\mathrm{Nd}_{0.40}\mathrm{NiO}_3$ (SNNO), and NdNiO_3 (NNO) films are textured on the (00l) oriented LaAlO_3 substrate. Thicknesses are, respectively, 17 ± 3 nm, 52 ± 5 nm, and 75 ± 5 nm. A transmission electronic microscopy study of the SNO film (not shown) testifies an atomically flat and coherent interface.

The temperature-dependent electrical characterization of the thin films was measured from −270 to 250 °C by the well-known four-probe technique[26] using a dc current and platinum wires with a conducting silver paint (Ag epoxy, each separated by 0.5 mm). The surface of the contacts is about 0.5 mm^2. The value of the measured resistance is obtained by the average of four measurements at different currents injected by a precision current source Keitley 6220 on the external electrodes. A nanovoltmeter Keitley 2182A was used to measure the voltages across the electrical leads, with two internal probes, to obtain the resistance of the sample. The resistivity ρ is calculated from the resistance R by using

$$\rho = \frac{\pi w}{\ln 2} R,$$

with w being the thickness of the film.[27] Figure 1 shows the temperature-induced evolution of the resistivity for different rare earth nickelate thin films and illustrates that all three films undergo a MI transition at T_{MI} and that T_{MI} depends critically on the size of the rare earth. The observed T_{MI}s are determined from the point of deflection of the resistivity curve at 120 °C (SNO), 45 °C (SNNO), and −115 °C (NNO, on heating). These values differ from the values reported in literature on bulk samples; the difference can be attributed to the effect of strain in the thin films. In agreement with literature, the resistivity curve of NNO presents a hysteresis indicating a first-order phase transition; such a hysteresis is not observed for SNO and SNNO.

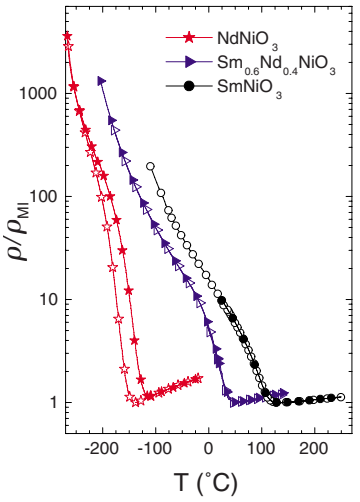

FIG. 1. (Color online) Resistivity vs temperature for different rare earth nickelate thin films [SmNiO_3 (SNO, ●/○), $\mathrm{Sm}_{0.60}\mathrm{Nd}_{0.40}\mathrm{NiO}_3$ (SNNO, ▶/▷), and NdNiO_3 (NNO, ★/☆)]. The full and open signals correspond to heating and cooling, respectively. ρ_{MI} is the resistivity at T_{MI}.

Raman spectra were recorded with a LabRam Jobin-Yvon spectrometer. The 514.5 nm line of an Ar^+ ion laser was used as excitation line. Experiments were conducted in micro-Raman; the light was focused to a 1 $\mu\mathrm{m}^2$ spot. All measurements performed under the microscope were recorded in a back-scattering geometry; the instrumental resolution was 2.8 ± 0.2 cm^{-1}. It has been reported earlier that Raman spectra recorded on black manganite[20,28] and nickelate thin films[18] can show a strong dependence on the exciting laser power. As a consequence, standard experiments have been carried out using low powers (less than 1 mW under the microscope, using a times 50lf objective) and it has been verified that no structural transformations and overheating take place. Namely, the below discussed difference in T_{MI} between Raman scattering and conductivity measurements and between bulk and thin-film data do not result from laser heating. Temperature-dependent Raman measurements have been carried out by using a commercial LINKAM heating stage placed under the Raman microscope. After an initial cooling, all presented spectra have been obtained by heating the sample from low temperature (−180 °C) above room temperature (up to 150 °C), this is in the following simplified as "heating." The Raman spectra before and after temperature measurements are identical, attesting the reversibility of temperature-induced changes.

III. RAMAN SCATTERING OF $Sm_{1-x}Nd_xNiO_3$ THIN FILMS

A. General considerations

The high-temperature metallic phase of *R* nickelates is an orthorhombically distorted perovskite with space group *Pbnm*. With respect to the ideal cubic $Pm\bar{3}m$ perovskite structure the orthorhombic structure is obtained by an antiphase tilt of the adjacent NiO_6 octahedra ($a^-a^-c^+$ in Glazer's notation[29]). *R* nickelates are thus ferroelastic. The 10 atoms in the unit cell of the orthorhombic structure give rise to 24 Raman-active modes[18]

$$\Gamma_{\mathrm{Raman},Pbnm(\mathrm{metallic})} = 7A_{1g} + 7B_{1g} + 5B_{2g} + 5B_{3g}.$$

The proposed[5,6] low-temperature monoclinic structure of *R* nickelates (space group $P2_1/n$) presents also 24 Raman-active modes

$$\Gamma_{\mathrm{Raman},P2_1/n(\mathrm{insulator})} = 12A_g + 12B_g.$$

As a consequence of this, the number of Raman bands alone does not allow distinguishing between the orthorhombic and monoclinic space groups, but changes in the spectral signature are expected to mirror any change in symmetry. To date Raman scattering data on *R* nickelates remain still limited in the literature and the authors are only aware of a temperature-dependent investigation of $NdNiO_3$ (Ref. 18) and a room-temperature spectrum of $SmNiO_3$ (Ref. 22).

B. Room-temperature spectra

Let us first remind that NNO is at room-temperature metallic (orthorhombic), SNO is insulating (expected monoclinic), and SNNO is close to the metal-insulator transition. Figure 2 presents a comparison of room-temperature Raman spectra for SNO, SNNO, and NNO. The spectrum of NNO is similar to the data reported in the literature[18] and clearly distinct from the SNO spectrum, suggesting that NNO and SNO do not adopt the same crystal structure at room temperature. It can also be seen that the Raman signature of SNNO is rather similar to that of NNO which in turn suggest that SNNO is orthorhombic at room temperature.

C. Temperature-dependent Raman scattering

Figure 3 presents temperature-dependent Raman spectra for SNO, NNO, and SNNO while Fig. 4 shows how the band positions change with temperature for SNO and SNNO.

The spectra of NNO are similar to those previously reported in Ref. 18. Although the low-wave-number soft mode is not observed due to the Notch-filter cutoff of our spectrometer a phase transition around $T_{\mathrm{MI}}=T_N=-115$ °C is evidenced by significant changes in the spectral signature. When going from low to high-temperature one notices, namely, (i) the change from of one strong band ($\approx$300 cm^{-1}) and one weak band ($\approx$330 cm^{-1}) toward a new single band around ($\approx$310 cm^{-1}), (ii) a sudden low-wave-number shift of some of the bands around 420 cm^{-1}, and (iii) a disappearance of the bands around 400 cm^{-1}.

All these features of Fig. 3(c) are clear evidences for a structural phase transition of NNO at T_{MI}. Raman scattering

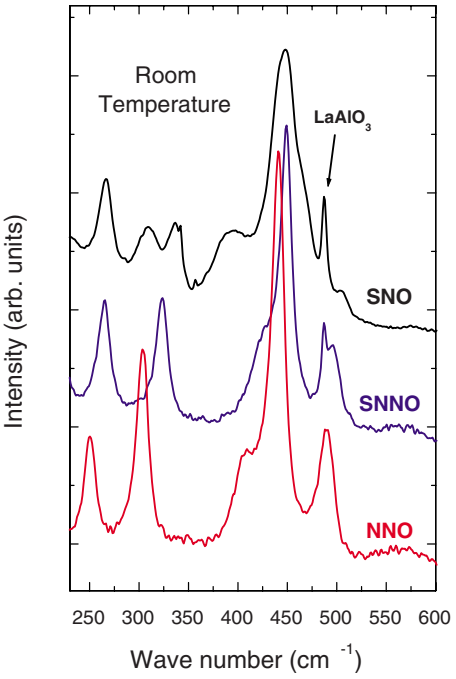

FIG. 2. (Color online) Comparison of room-temperature Raman spectra for $SmNiO_3$, $Sm_{0.60}Nd_{0.40}NiO_3$, and $NdNiO_3$. The arrows indicate Raman bands from the $LaAlO_3$ substrate.

on its own does not allow the determination of the two space groups but it is likely that the signature corresponds to the transition proposed in literature[9,10,18] when heating NNO: monoclinic $P2_1/n \rightarrow$ orthorhombic *Pbnm*. We further note that a phase coexistence is observed at T_{MI} as, namely, evidenced by the presence of both the "monoclinic" band at 300 cm^{-1} and the "orthorhombic" band at 310 cm^{-1} at the critical temperature. This is in agreement with, and further evidence of, a first-order phase transition of NNO at T_{MI}. When the temperature is further increased in the metallic phase up to room temperature the Raman signature presents no changes apart from a slight temperature shift due to thermal expansion and thermal broadening of all bands.

We will now discuss the temperature-dependent signature of SNO. At a low-temperature of −180 °C SNO is an antiferromagnetic insulator and the Raman signature of SNO is similar to that of NNO, which suggests that SNO and NNO adopt the same crystal structure. Since bulk NNO is reported[18] to be monoclinic at low temperature this similarity suggests that SNO also adopts a monoclinic structure in the low-temperature range below T_{MI}. Upon heating SNO enters at T_N the paramagnetic phase where it shows first significant changes in its Raman spectra. It can be seen in Figs. 3(a) and 4 that the band at initially 420 cm^{-1} shows from T_N to T_{MI} a significant softening of 30 cm^{-1} toward lower wave numbers. Furthermore, a decrease in intensity (relative to the massif at 450 cm^{-1}) and an increase in its width of the same band are observed. Although this softening is the predominant signature of the intermediate paramagnetic-insulator phase other less visible spectral changes such as the progressive intensity loss of the band at 320 cm^{-1} (relative to the massif at 450 cm^{-1}) accompany the spectral evolution. The possible origins of the softening are discussed in more detail

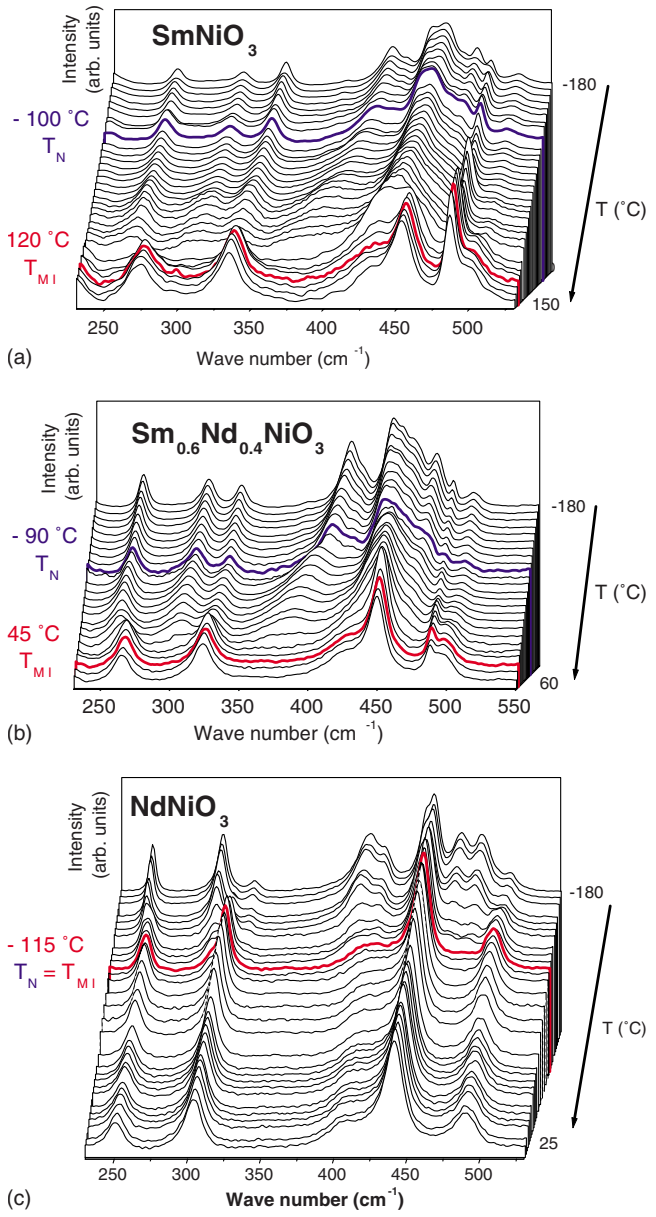

FIG. 3. (Color online) Selected temperature-dependent Raman spectra for $SmNiO_3$ (top), $Sm_{0.60}Nd_{0.40}NiO_3$ (middle), and $NdNiO_3$ (bottom). The displayed spectra have been obtained by heating from −180 °C with a step of 5 °C; for simplicity only every second spectrum is shown. The red spectra correspond to MI-transition temperatures (deduced from Fig. 1), while the blue spectra correspond to magnetic Néel-transition temperatures (bulk literature data). Note that T_{MI} measured by the electrical four-probe technique (in red) is by roughly 20 °C higher than the observed anomalies in the Raman spectra (see text).

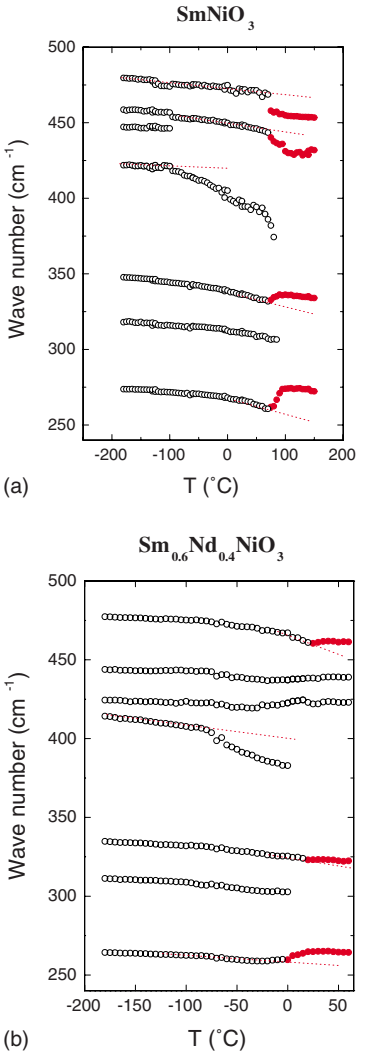

FIG. 4. (Color online) Temperature-dependent evolution of the band position in the Raman spectra of (a) $SmNiO_3$ and (b) $Sm_{0.60}Nd_{0.40}NiO_3$. Lines and colors are guides to the eye to emphasize spectral changes which in turn are evidences for a structural phase transition at T_{MI} (see text).

in the discussion Sec. IV. When the temperature is now further increased SNO enters at T_{MI} the paramagnetic-metallic phase where new significant changes in the spectral signature are observed. Three changes are predominant (Figs. 3 and 4): (i) the suppression of the above-described 420 cm^{-1} mode and the band at initially 320 cm^{-1}, (ii) an abrupt change in wave number of the band at initially 270 cm^{-1}, and (iii) a significant change in the intensity distribution of the massif between 400 and 450 cm^{-1}. Again all these spectral changes offer direct evidence for a structural phase transition at T_{MI}, which most likely corresponds to a transition from a low-temperature monoclinic phase to the well-known *Pbnm* orthorhombic phase above T_{MI}.

Although the electrical and Raman measurements are done on physically the same thin film, the T_{MI} measured by Raman scattering is roughly 20 °C lower than what is observed with the electrical four-probe technique. This observation is likely due to the fact that Raman scattering is a local probe while the electric measurement probes a macroscopic phase transition. In agreement with literature, this apparent discrepancy between electrical and Raman measurements offers thus further hints for local structural/electric deviations from the average structure in *R* nickelates.

Having discussed the spectral signatures of $SmNiO_3$ and $NdNiO_3$, it is now interesting to inspect the signature of a member of the solid solution $Sm_{0.60}Nd_{0.40}NiO_3$. It can be seen from Fig. 3(b) that the overall evolution of the Raman spectra of SNNO with temperature is very similar to SNO

but different from NNO. Note that the temperature range of the intermediate paramagnetic-insulator phase ($T_N < T < T_{MI}$), by using the range of the mode softening as an indicator, extends over a smaller temperature range for SNNO when compared to SNO, in agreement with earlier results from electric and magnetic measurements.[2,15]

IV. DISCUSSION

It has been shown in Sec. III that the temperature-dependent Raman signature through the MI transition is different for a R nickelate where $T_{MI}=T_N$ (NNO) compared to those where $T_{MI}\neq T_N$ (SNO and SNNO). The difference is revealed by the observation that the paramagnetic-insulator phase (which only exists in the $T_{MI}\neq T_N$ systems) has a specific Raman signature. The predominant signature is a mode at $\approx$420 cm^{-1}, which softens significantly to lower wave numbers when the antiferromagnetic-paramagnetic phase transition at T_N is crossed upon heating, leading to an important shift of 30–40 cm^{-1} between T_N and T_{MI}, thus in the paramagnetic-insulating phase (Fig. 5). This pronounced softening indicates an important anharmonicity which cannot be explained by a classical temperature behavior but points at a further contribution. A straightforward interpretation of this softening is difficult because a number of different explanations might be considered. The aim of the following part will be to illustrate different possible origins and to cut the discussion down to the most likely scenarios.

At first sight, the considerable spectral changes at T_N for SNO and SNNO could be an indication of a structural rearrangement which has to be subtle or to occur on a local level since it is not detected by x-ray or neutron diffraction. Although we cannot formally exclude a change in the space group at T_N, such a scenario is very unlikely due the absence of a new spectral signature in terms of new bands, band splitting, etc. Given the fact that the softening starts at T_N, one should consider magnetostriction. However, the usually observed changes in lattice parameter at T_N are by far too small to cause the observed phonon anomaly, especially over a broad range of temperature.

It is useful to recall that the important softening is mainly observed for one band, which indicates that a particular type of chemical bonding (and its associated force constant) changes with temperature. In perovskites, the spectral region of this band is usually associated with vibrations of the octahedron and, in agreement with literature,[18] we thus attribute the 420 cm^{-1} band to a mode involving distortions of the NiO_6 octahedra which in turn is a signature for significant changes in the Ni-O bonding. This brings us back to the fact that it has been proposed that the Ni-O bonding is considerably modified at T_{MI}, whereof one proposed mechanism is the following charge dispropornation upon cooling:

$$2Ni^{3+}(\text{metallic, orthorhombic}) \rightarrow Ni^{3+\delta} + Ni^{3-\delta}(\text{insulating, monoclinic}).$$

Such a mechanism conditions on a local level a significant change in chemical bonding since the charge dispropornation leads to an increased covalent character of the Ni-O bond.

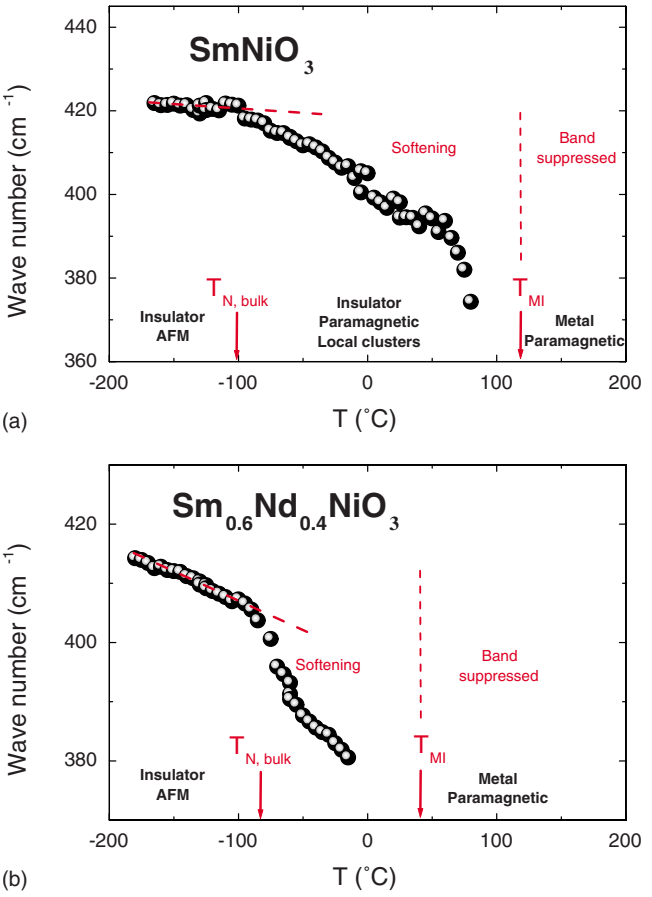

FIG. 5. (Color online) Temperature-dependent evolution of the band showing a significant softening for (a) $SmNiO_3$ and (b) $Sm_{0.60}Nd_{0.40}NiO_3$. Lines and colors are guides to the eye to underline spectral changes at the magnetic (T_N) and electronic (T_{MI}) phase transitions, see text for more details. T_N corresponds to literature results on bulk samples, while T_{MI} corresponds to the measured metal-insulator phase transition on physically the same films which have been investigated by Raman scattering.

The charge order, i.e., the magnitude of δ, has been earlier proposed[30] to be the order parameter close to the MI transition. Within this picture it appears natural to consider that the softening of the band at 420 cm^{-1} might be the signature of a temperature-dependent increase of the charge dispropornation, i.e., δ increases with decreasing temperature up to the magnetic phase transition from whereof it is rather stabilized. However, to the best of our knowledge, there is no example in the literature where a change in a charge dispropornation alone has conditioned a large phonon softening.

Finally, a possible coupling between spin and phonon degrees of freedom can be considered. A useful approach for the understanding of spin-dependent phonon frequencies is based on an initial model by Baltensperger and Helman[31] where it has been proposed that the phonon frequencies in magnetic materials are affected by the correlation of nearest-neighbor spin pairs.[31,32] Such a scenario should be considered to explain also the observed anomaly in SNO and SNNO but the amplitude of the here reported softening remains large compared to what is known for other magnetic materials, e.g., the structurally similar orthoferrite $EuFeO_3$

presents at its AFM-PM phase transitions a phonon anomaly of an order of magnitude smaller than what we observe for SNO.[33] The spin-phonon coupling in other materials such as MF_2 (M=Fe, Mn),[32] $Y_2Ru_2O_7$ (Ref. 34), $LaTiO_3$ (Ref. 35), or $ZnCr_2O_4$ (Ref. 36) is also significantly smaller than in our observation.

Nevertheless, we believe that the observation of the anomaly around T_N suggests that spin-phonon coupling is a contributing mechanism but it is unlikely that spin-phonon coupling alone can explain the observed softening. We thus consider a coupling to another order parameter which does change with temperature. One common order parameter in perovskites is cation displacement thus ferroelectricity. As mentioned in Sec. I, recent reports propose that R nickelates present in their insulator phase a charge-order driven (thus improper) ferroelectricity due to the polar displacements of Ni cations.[4,7,8] Other authors discuss the possibility of potential ferroelectricity in the antiferromagnetic E phase of the orthorhombic ground state of nickelates.[7,37] Ferroelectric soft modes usually occur at lower wave numbers. On the other hand, the remarkable softening observed in SNO and SNNO might be related to the fact that both magnetic and ferroelectric orders coexist and are temperature dependent at the same time. This allows drawing the following tentative scenario: The onset of magnetic correlations takes place within a temperature regime that presents ferroelectric lattice instabilities, i.e., in a regime where the Ni cations are easily displaced in response to any perturbation (here magnetic correlations). This scenario is consistent with our assignment of the softening band to distortions of the NiO_6 octahedra (thus Ni-O bonding). This scenario calls for two notes: First, our observed softening extends deep into the paramagnetic phase thus it has to be primarily driven by *local* magnetic correlations; as stated in Sec. I such a local (clusterlike) structure is commonly accepted for R nickelates.[11–14] Second, the local structure is, namely, characterized by changes in the charge order (in magnitude and size) which in turn drives the hypothetical ferroelectricity. As a consequence, one can expect an intimate correlation between magnetism, charge order, and ferroelectricity in this highly correlated electron system. The above-described coupling, however, is a hypothesis which remains to be elucidated, namely, by ferroelectric measurements which are unfortunately (further to conductivity problems) not straightforward for films on an insulating substrate as is the case for the here investigated samples.

V. CONCLUSION

$SmNiO_3$, $NdNiO_3$, and $Sm_{0.60}Nd_{0.40}NiO_3$ thin films have been investigated by temperature-dependent Raman scattering across their magnetic and MI transitions. The spectral signature provides evidence that all investigated samples present a structural phase transition at T_{MI}. Interestingly, the Raman signature across T_{MI} is significantly different for $NdNiO_3$ ($T_{MI}=T_N$) compared to $SmNiO_3$ and $Sm_{0.60}Nd_{0.40}NiO_3$ ($T_{MI}\neq T_N$), thus suggesting that the mechanisms are not the same. It has been observed that the paramagnetic-insulator phase ($T_N<T<T_{MI}$) in $SmNiO_3$ and $Sm_{0.60}Nd_{0.40}NiO_3$ is characterized by a pronounced softening of one particular phonon band around 420 cm^{-1}. This signature is unusual and points to important and continuous modifications in Ni-O bonding, which stabilize upon cooling at the magnetic transition. The observed behavior might well be a general feature for all rare earth nickelates with $T_{MI}\neq T_N$.

We relate this softening to spin-phonon coupling and hypothesize that a coupling to a ferroelectric order-parameter conditions the unusual strength of the softening. In this scenario the softening is thus directly related to the theoretically[4,7,8] predicted magnetoelectric multiferroic character of the insulating regime in SNO and SNNO and would be the first experimental hint that R nickelates are indeed multiferroic. More experimental and theoretical works are needed to unambiguously identify the physical mechanisms leading to the anomalies reported here and to confirm the multiferroic character. First-principles calculations of the phonon spectrum with models including magnetic correlations, the peculiar local structure, as well as lattice instabilities could lead to a better understanding of the proposed coupling.

ACKNOWLEDGMENTS

This work was supported by the European Network of Excellence FAME (Functionalized Advanced Materials and Engineering), by Schneider Electric S.A., and the European Strep MaCoMuFi. The authors thank H. Roussel (from the "Consortium des Moyens Technologiques Communs," CMTC) for x-ray characterization and A. Pasturel (SIMAP, Grenoble) for enlightening discussion on metal-insulator transitions. J. Marcus (Institut Néel, Grenoble) is acknowledged for access to electric transport measurements.

*Corresponding author: kreisel@inpg.fr

[1] G. Demazeau, A. Marbeuf, M. Pouchard, and P. Hagenmuller, J. Solid State Chem. **3**, 582 (1971).
[2] J. B. Torrance, P. Lacorre, A. I. Nazzal, E. J. Ansaldo, and Ch. Niedermayer, Phys. Rev. B **45**, 8209 (1992).
[3] M. L. Médarde, J. Phys.: Condens. Matter **9**, 1679 (1997).
[4] G. Catalan, Phase Transitions **81**, 729 (2008).
[5] J. A. Alonso, J. L. García-Muñoz, M. T. Fernández-Díaz, M. A. G. Aranda, M. J. Martínez-Lope, and M. T. Casais, Phys. Rev. Lett. **82**, 3871 (1999).
[6] J. A. Alonso, M. J. Martínez-Lope, M. T. Casais, J. L. García-Muñoz, and M. T. Fernández-Díaz, Phys. Rev. B **61**, 1756 (2000).
[7] S. W. Cheong and M. Mostovoy, Nat. Mater. **6**, 13 (2007).
[8] J. V. d. Brink and D. I. Khomskii, arXiv:0803.2964v3, J. Phys.: Condens. Matter (to be published).
[9] U. Staub, G. I. Meijer, F. Fauth, R. Allenspach, J. G. Bednorz, J. Karpinski, S. M. Kazakov, L. Paolasini, and F. d'Acapito, Phys.

Rev. Lett. **88**, 126402 (2002).
[10] V. Scagnoli, U. Staub, M. Janousch, A. M. Mulders, M. Shi, G. I. Meijer, S. Rosenkranz, S. B. Wilkins, L. Paolasini, J. Karpinski, S. M. Kazakov, and S. W. Lovesey, Phys. Rev. B **72**, 155111 (2005).
[11] J.-S. Zhou and J. B. Goodenough, Phys. Rev. B **69**, 153105 (2004).
[12] J.-S. Zhou, J. B. Goodenough, and B. Dabrowski, Phys. Rev. B **67**, 020404(R) (2003).
[13] J. Pérez-Cacho, J. Blasco, J. Garcia, M. Castro, and J. Stankiewicz, J. Phys.: Condens. Matter **11**, 405 (1999).
[14] C. Piamonteze, H. C. N. Tolentino, A. Y. Ramos, N. E. Massa, J. A. Alonso, M. J. Martínez-Lope, and M. T. Casais, Phys. Rev. B **71**, 012104 (2005).
[15] A. Ambrosini and J.-F. Hamet, Appl. Phys. Lett. **82**, 727 (2003).
[16] P. Zhang, T. Haage, H.-U. Habermeier, T. Ruf, and M. Cardona, J. Appl. Phys. **80**, 2935 (1996).
[17] C. Thomsen, R. Wegerer, H. U. Habermeier, and M. Cardona, Solid State Commun. **83**, 199 (1992).
[18] M. Zaghrioui, A. Bulou, P. Lacorre, and P. Laffez, Phys. Rev. B **64**, 081102(R) (2001).
[19] J. Kreisel, S. Pignard, H. Vincent, J. P. Senateur, and G. Lucazeau, Appl. Phys. Lett. **73**, 1194 (1998).
[20] J. Kreisel, G. Lucazeau, C. Dubourdieu, M. Rosina, and F. Weiss, J. Phys.: Condens. Matter **14**, 5201 (2002).
[21] M. A. Novojilov, O. Y. Gorbenko, I. E. Graboy, A. R. Kaul, H. W. Zandbergen, N. A. Babushkina, and L. M. Belova, Appl. Phys. Lett. **76**, 2041 (2000).
[22] N. Ihzaz, S. Pignard, J. Kreisel, H. Vincent, J. Marcus, J. Dhahri, and M. Oumezzine, Phys. Status Solidi C **1**, 1679 (2004).
[23] C. Girardot, F. Conchon, A. Boulle, P. Chaudouet, N. Caillault, J. Kreisel, F. Weiss, and S. Pignard, Surf. Coat. Technol. **201**, 9021 (2007).
[24] F. Conchon, A. Boulle, C. Girardot, S. Pignard, R. Guinebretière, E. Dooryhée, J.-L. Hodeau, F. Weiss, J. Kreisel, and J.-F. Bérar, J. Phys. D **40**, 4872 (2007).
[25] F. Conchon, A. Boulle, R. Guinebretière, C. Girardot, S. Pignard, J. Kreisel, F. Weiss, E. Dooryhée, and J.-L. Hodeau, Appl. Phys. Lett. **91**, 192110 (2007).
[26] E. Hesse, Solid-State Electron. **21**, 637 (1978).
[27] A. E. Stephens, H. J. Mackey, and J. R. Sybert, J. Appl. Phys. **42**, 2592 (1971).
[28] M. N. Iliev, M. V. Abrashev, H. G. Lee, V. N. Popov, Y. Y. Sun, C. Thomsen, R. L. Meng, and C. W. Chu, Phys. Rev. B **57**, 2872 (1998).
[29] A. M. Glazer, Acta Crystallogr., Sect. B: Struct. Crystallogr. Cryst. Chem. **28**, 3384 (1972).
[30] F. P. de la Cruz, C. Piamonteze, N. E. Massa, H. Salva, J. A. Alonso, M. J. Martínez-Lope, and M. T. Casais, Phys. Rev. B **66**, 153104 (2002).
[31] W. Baltensperger and J. S. Helman, Helv. Phys. Acta **41**, 668 (1968).
[32] D. J. Lockwood and M. G. Cottam, J. Appl. Phys. **64**, 5876 (1988).
[33] R. Haumont, J. Kreisel, and P. Bouvier, Phase Transitions **79**, 1043 (2006).
[34] J. S. Lee, T. W. Noh, J. S. Bae, I.-S. Yang, T. Takeda, and R. Kanno, Phys. Rev. B **69**, 214428 (2004).
[35] M. N. Iliev, A. P. Litvinchuk, M. V. Abrashev, V. N. Popov, J. Cmaidalka, B. Lorenz, and R. L. Meng, Phys. Rev. B **69**, 172301 (2004).
[36] A. B. Sushkov, O. Tchernyshyov, W. Ratcliff, S.-W. Cheong, and H. D. Drew, Phys. Rev. Lett. **94**, 137202 (2005).
[37] I. A. Sergienko, C. Sen, and E. Dagotto, Phys. Rev. Lett. **97**, 227204 (2006).